

# Identifying the Proper Impedance Plane and Fault Trajectories in Distance Protection Analysis

Fernando Calero and Héctor J. Altuve  
*Schweitzer Engineering Laboratories, Inc.*

Presented at the  
66th Annual Georgia Tech Protective Relaying Conference  
Atlanta, Georgia  
April 25–27, 2012

Originally presented at the  
38th Annual Western Protective Relay Conference, October 2011

# Identifying the Proper Impedance Plane and Fault Trajectories in Distance Protection Analysis

Fernando Calero and Héctor J. Altuve, *Schweitzer Engineering Laboratories, Inc.*

**Abstract**—Distance relay characteristics have long been discussed in literature, but with little regard to the impedance plane to which they refer. Numerical distance relays include phase and ground elements with different characteristics. They also include power swing detection, load encroachment, and directional elements that generally require different impedance planes than those used for distance elements.

This paper centers on the selection of the impedance plane for analyzing the operation of distance, power swing detection, and directional elements. With simple power system models, this paper shows element characteristics and impedance loci and trajectories on different planes to explain the concepts and discuss practical applications. This paper also describes a real power system disturbance and illustrates the use of different impedance planes for analyzing protection element operation.

## I. INTRODUCTION

Distance protection generally requires six elements (AB, BC, CA, AG, BG, and CG) to protect against the ten possible fault types. These elements are continuously monitoring the power system. In most cases, more than one element may operate for a given fault or other abnormal condition. In general, both the distance element characteristics and the impedances measured during faults depend on the fault type and the pre-fault system operating conditions.

The impedance or R-X plane has been traditionally used to analyze distance element operation for different power system conditions, such as faults, power swings, and load conditions [1] [2] [3] [4]. This method of analysis requires the element operating characteristic and the impedance measured by the element for the given power system condition to be plotted on the same plane. The element operates when the measured impedance falls in the operating region of its characteristic.

For unbalanced faults, more than one impedance plane can be used to analyze distance element operation. For example, the operation of the BC distance element for a CA fault can be analyzed on the ZBC impedance plane or the ZCA impedance plane. The element characteristic and the measured impedance look different on both planes. Many publications address distance element characteristics and measured impedances but do not explicitly discuss the impact of the plane selected for analysis.

Multifunction line protection relays have fault selectors that enable only the appropriate distance elements for a given fault [5] [6]. Electromechanical protection schemes have standalone relays with OR tripping logic [1]. It is important to understand the practical impact of the presence or absence of

fault type selection logic on the characteristic that the distance relay presents to a fault. This knowledge is also important to properly test distance relays.

Distance relays typically include directional elements. In many cases, these directional elements respond to different quantities (for example, negative- or zero-sequence quantities) from those of the distance elements. In one implementation, the directional elements measure the negative- or zero-sequence impedance [7]. A common misconception is to try to represent directional element characteristics on the same plane used for distance elements.

Multifunction relays include other protection elements, such as power swing detection and load-encroachment elements, that typically respond to positive-sequence quantities. These elements require a positive-sequence impedance plane for analysis, instead of the plane used for distance elements.

This paper focuses on the proper selection of the impedance plane for analyzing the operation of distance, directional, and other protection elements. Using computer simulation results from simple power system models, the paper shows element characteristics and impedance loci and trajectories on different planes to explain the concepts and discuss practical applications.

## II. IMPEDANCE PLANES

A way to analyze the operation of two-input protection elements is to use a complex plane defined by the ratio of the input signals. Two planes have been mainly used in protective relaying: the impedance plane and the current-ratio plane. The admittance plane, an alternative to the impedance plane, is seldom used.

The impedance plane is a tool to analyze distance, directional, and power swing detection element operation by superimposing element operating characteristics and the measured impedances for various power system conditions, including faults, power swings, and normal load conditions.

### A. Impedance Planes for Distance Elements

#### 1) Measured or Apparent Impedance

Distance elements respond to voltage (V) and current (I) signals measured at their location in the power system. These elements perform phase or amplitude comparison of signals derived from V and I to create operating characteristics [3] [4] [6] [7] [8] [9].

Conceptually, dividing the measured voltage phasor  $V$  by the measured current phasor  $I$  yields the impedance  $Z$  measured by the distance element, or apparent impedance, which serves to analyze distance element operation.

$$Z = \frac{V}{I} \quad (1)$$

This apparent impedance can be plotted on a complex impedance plane. The set of  $Z$  values for which a distance element is on the verge of operation plots on the impedance plane as the element operating characteristic, which divides the operating region from the restraining region.

The distance element is constantly receiving its input voltage and current signals and conceptually deriving a  $Z$  value under all operating conditions of the power system. In steady state (a fixed load condition or a fault after the transient has died out),  $Z$  plots as a point on the impedance plane. During transient events (such as a power swing or the transient stage of a fault or of the relay measurement process),  $Z$  describes a trajectory. The distance element operates when the point or trajectory stays in the operating region of its characteristic for longer than the element operating time.

As mentioned previously, line distance protection generally requires at least six distance elements. Distance element input signals  $V$  and  $I$  should be such that, for any forward fault type, at least one element measures the positive-sequence impedance between the relay and the fault. This impedance is a measure of the distance to the fault. The appropriate  $V$  and  $I$  signals can be derived using symmetrical components.

Fig. 1 shows the positive-sequence network that represents a forward bolted (no fault resistance) three-phase fault in a radial system. The three-phase fault is simple to visualize and can be used to illustrate concepts. In Fig. 1 and the rest of this paper,  $V$  is the measured voltage phasor,  $I$  is the measured current phasor,  $ZL$  is the line impedance,  $ZS$  is the source impedance, and  $VF$  is the voltage phasor at the fault point. Equation (2) shows that several voltage and current combinations provide an impedance measurement equal to the positive-sequence impedance  $ZL1$  for this fault.

$$ZL1 = \frac{V1}{I1} = \frac{VA}{IA} = \frac{VB}{IB} = \frac{VC}{IC} = \frac{VAB}{IAB} = \frac{VBC}{IBC} = \frac{VCA}{ICA} \quad (2)$$

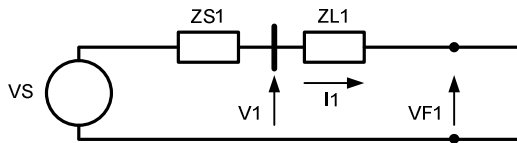


Fig. 1. Symmetrical component network for a bolted three-phase fault.

Fig. 2 depicts the sequence network for a forward bolted phase-to-phase (BC) fault. Fig. 2 shows that  $VF1 = VF2$ , which is used to find an expression for  $ZL1$ . Equation (3) gives the voltage and current combinations that provide an impedance measurement equal to  $ZL1$  for these faults. This expression is also valid for ABC and BCG faults.

$$ZL1 = \frac{V1 - V2}{I1 - I2} = \frac{VBC}{IBC} \quad (3)$$

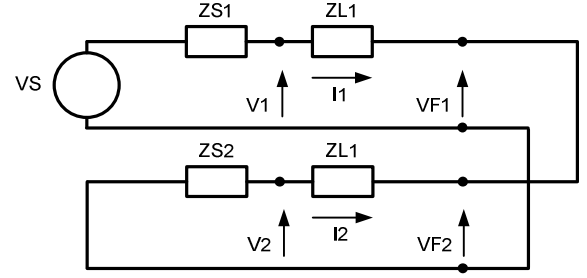


Fig. 2. Symmetrical component network for a bolted phase-to-phase fault.

Fig. 3 depicts the sequence network for a forward bolted single-phase-to-ground (AG) fault. Fig. 3 shows that  $VF1 + VF2 + VF0 = 0$ , which is used to find an expression for  $ZL1$ . Measuring  $ZL1$  for this fault requires measuring the A-phase voltage and a compensated A-phase current, as (4), (5), and (6) show. Equation (5) is also valid for ABC, ABG, and CAG faults.

$$ZL1 = \frac{V1 + V2 + V0}{I1 + I2 + I0 + \left(\frac{ZL0 - ZL1}{3ZL1}\right)3I0} \quad (4)$$

$$ZL1 = \frac{VA}{IA + k0 \cdot 3I0} \quad (5)$$

$$k0 = \frac{ZL0 - ZL1}{3ZL1} \quad (6)$$

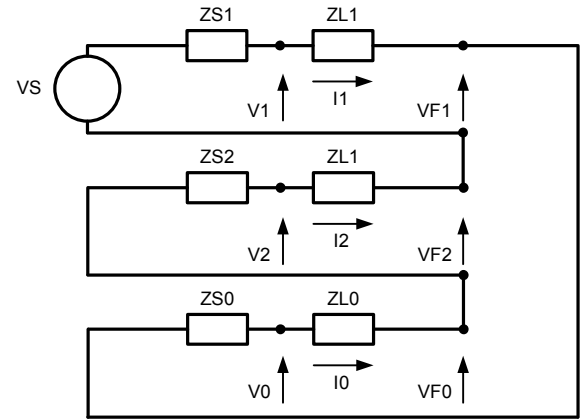


Fig. 3. Symmetrical component network for a bolted single-phase-to-ground fault.

From (2), (3), and (5), we conclude that six distance elements with the input signals shown in Table I provide protection for all ten possible fault types. For bolted faults, the phase and ground elements that receive only faulted phase information (referred to as the fault loop elements) measure the positive-sequence impedance between the relay and the fault. Table I also shows the fault types for which each element measures the correct positive-sequence impedance for bolted faults.

TABLE I  
VOLTAGE AND CURRENT INPUT SIGNALS TO TRADITIONAL PHASE AND  
GROUND DISTANCE ELEMENTS

Distance Elements	Voltage (V)	Current (I)	Fault Types	
Phase Elements	AB	VA – VB	IA – IB	ABC, AB, ABG
	BC	VB – VC	IB – IC	ABC, BC, BCG
	CA	VC – VA	IC – IA	ABC, CA, CAG
Ground Elements	AG	VA	IA + k0 • 3I0	ABC, ABG, CAG, AG
	BG	VB	IB + k0 • 3I0	ABC, ABG, BCG, BG
	CG	VC	IC + k0 • 3I0	ABC, BCG, CAG, CG

However, distance elements that receive unfaulted phase information measure impedances that are different from the line section impedance between the relay and the fault [1] [2] [3] [4].

### 2) Impedance Plane Alternatives

The six impedance measurement loops shown in Table I define six possible impedance planes: ZAB, ZBC, ZCA, ZAG, ZBG, and ZCG. To analyze, for example, the response of the BC distance element to a CA fault, we can use the ZBC plane or the ZCA plane. The ZBC plane in this example is the apparent impedance plane, and the ZCA plane is the fault loop impedance plane.

The apparent impedance plane is a plot of the impedance  $Z$  measured by the distance element, given by (1). This plane represents the ratio of the element voltage and current input (or measured) signals. The polarity or direction assumed as positive for the currents in the distance element equations determines the forward direction of the apparent impedance. In our previous example, the apparent impedance plane for the BC element is a plot of the ratio of  $V = VB - VC$  to  $I = IB - IC$ .

The apparent impedance plane is the best plane to analyze distance element operation because it allows the representation of the element operating characteristics and the measured impedances for faults, power swings, and load conditions. The characteristics provided by relay manufacturers are shown on this plane for nonfault conditions and look like static characteristics. The characteristics obtained when testing a distance relay also correspond to this plane.

The fault loop impedance plane is a plot of the ratio of the voltage and current corresponding to the faulted phases (instead of the element input signals). In our example, the fault loop impedance plane for the CA fault is a plot of the ratio of  $VC - VA$  to  $IC - IA$ .

Section III shows that a distance element characteristic and the impedance measured by this element for a given fault look different on both planes. Section III also shows that it is sometimes convenient for the characteristics and impedances measured by distance elements from different phases to be represented on the same plane.

## B. Other Impedance Planes

### 1) Positive-Sequence (V1/I1) Impedance Plane

In some relays, power swing detection, load encroachment, and some directional elements respond to the positive-sequence voltages and currents [4] [6] [10]. Hence, the positive-sequence (V1/I1) impedance plane is the best tool to analyze the operation of these elements (see Section IV).

### 2) Negative-Sequence (V2/I2) and Zero-Sequence (V0/I0) Impedance Planes

Some directional elements respond to negative- or zero-sequence voltages and currents [7]. Negative- or zero-sequence impedance planes serve to analyze the operation of these elements (see Section V).

## III. APPARENT AND FAULT LOOP IMPEDANCE PLANES

### A. Distance Element Characteristics

Many distance elements are described in various publications. These elements differ in implementation and polarizing quantities. A phase mho distance element, polarized with positive-sequence voltage, is used as an example for our discussion of element characteristics.

A distance element performs the phase comparison of an operating quantity (S1) and a polarizing quantity (S2). The threshold operating condition generally occurs when the two phasors are in quadrature, as (7) shows.

$$\arg\left(\frac{S1}{S2}\right) = \arg\left(\frac{Z - \mathbf{a}}{Z - \mathbf{b}}\right) = \pm 90^\circ \quad (7)$$

Equation (7) describes a circle on the impedance ( $Z$ ) plane [8] [9]. The tips of phasors  $\mathbf{a}$  and  $\mathbf{b}$  determine the diameter of the circle (see Fig. 4 later in this paper). Hence, these phasors define the size and the position of the element characteristic on the impedance plane. Equation (7) defines the proper impedance plane to plot the element characteristic. For example, if  $Z = \frac{VB - VC}{IB - IC} = ZBC$ , the ZBC plane should be used.

### 1) Forward Faults

For forward faults, the distance element input currents flow in the tripping direction. Consider the BC mho distance element polarized with positive-sequence voltage. Equations (8) and (9) give the element input signals.

$$S1 = (VB - VC) - Zc(IB - IC) \quad (8)$$

$$S2 = (VB1 - VC1) \quad (9)$$

where:

$Zc$  is the setting that defines the mho element reach.

The ZBC plane is the apparent impedance plane for this BC mho element.

Dividing (8) and (9) by the current (to convert them into impedance equations), we obtain (10) and (11). Reference [8] describes the symmetrical component operations required to derive (11).

$$\frac{S1}{IB - IC} = \frac{VB - VC}{IB - IC} - Zc = ZBC - Zc \quad (10)$$

$$\begin{aligned} \frac{S2}{IB - IC} &= \frac{VB - VC}{IB - IC} - \frac{VB2 - VC2}{(IB1 - IC1) - (IB2 - IC2)} \\ &= ZBC - \frac{VB2 - VC2}{(IB1 - IC1) - (IB2 - IC2)} \end{aligned} \quad (11)$$

For a forward BC fault in a simple radial network, we obtain the  $\mathbf{a}$  and  $\mathbf{b}$  phasors from (7), (10), and (11) [8] [9]:

$$\mathbf{a} = Zc \quad (12)$$

$$\mathbf{b} = -\frac{ZS1}{2} \quad (13)$$

where:

$ZS1$  is the source positive-sequence impedance.

Fig. 4 shows the BC mho element characteristic for forward BC faults. This polarized mho element uses unfaulted phase information in the polarizing quantity by using the positive-sequence voltage. This polarizing quantity expands the circle to the third quadrant for forward faults. The mho characteristic has a fixed reach point, defined by the setting impedance  $Zc$ .

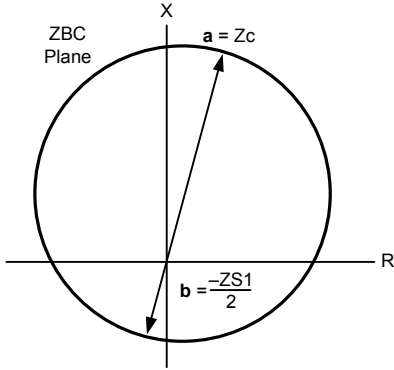


Fig. 4. BC polarized mho element characteristic for forward BC faults.

As mentioned previously, distance elements are constantly measuring currents and voltages. It is possible to find more generic expressions for  $\mathbf{a}$  and  $\mathbf{b}$ . Equations (14) and (15) provide the  $\mathbf{a}$  and  $\mathbf{b}$  expressions that determine polarized mho element characteristics for all operating conditions [8] [9]. Other distance elements will have similar expressions.

$$\mathbf{a} = Zc \quad (14)$$

$$\mathbf{b} = -ZS1 \left( \frac{1}{1 - \frac{IA1}{IA2}} \right) \quad (15)$$

Table II shows the  $\mathbf{b}$  phasor expressions for different types of forward faults in a simple unloaded radial network. Fig. 5

depicts the resulting BC element characteristics on the ZBC plane for the different types of forward faults. For the BC fault, the characteristic is the same as that in Fig. 4.

TABLE II  
b PHASOR VALUES FOR THE BC ELEMENT FOR DIFFERENT  
TYPES OF FORWARD FAULTS\*

Fault Type	IA1/IA2	$\mathbf{b}$
BG	$a^2$	$-ZS1/(1 - a^2)$
CG	$a$	$-ZS1/(1 - a)$
AB	$-a$	$ZS1/a^2$
BC	$-1$	$-ZS1/2$
CA	$-a^2$	$ZS1/a$

\* In Table II,  $a = e^{j120}$

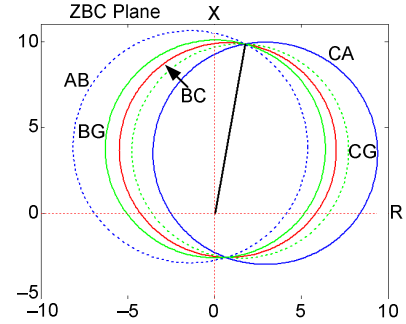


Fig. 5. BC element characteristics for different types of forward faults. The labels refer to fault types.

As mentioned previously, we can also use the fault loop impedance plane. As an example, Fig. 6 shows the characteristics of all the distance elements for a BC fault on the ZBC plane. In this example, the ZBC plane is the fault loop plane, and the characteristics of the distance elements receiving input signals from other phases differ from that of the faulted phase BC element. The BC element characteristic is the same as that in Fig. 4.

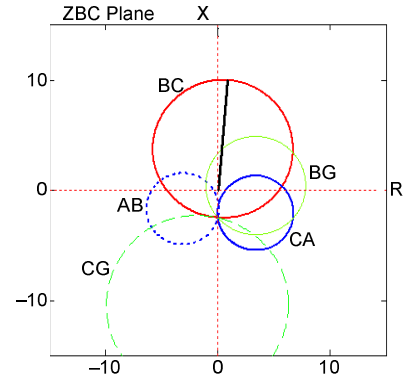


Fig. 6. Characteristics of all the distance elements on the ZBC plane for a forward BC fault. The labels refer to distance elements.

Most line protection relays use a faulted phase identification algorithm to supervise the distance elements. Some relays, for example, only enable the ground distance element of the faulted phase for single-phase-to-ground faults. For phase-to-phase-to-ground faults, the relay enables the phase distance element of the faulted phases [4] [5] [6]. As a

result, the relay presents only the characteristic corresponding to the faulted phases (for example, the characteristic for the BC fault in Fig. 4) and does not present all the other characteristics shown in Fig. 6. Electromechanical distance protection schemes consist of single-function relays with OR tripping logic and typically without any phase selection supervising logic. Hence, the scheme presents all the phase and ground element characteristics for all faults. The composite characteristic, therefore, looks similar to Fig. 6.

### 2) Reverse Faults

For a reverse BC fault, the distance element input currents flow in the nontripping direction. Equations (16) and (17) give the  $\mathbf{a}$  and  $\mathbf{b}$  phasors for reverse BC faults [8] [9]. The  $\mathbf{b}$  phasor has the opposite sign as that for forward faults.

$$\mathbf{a} = Z_c \quad (16)$$

$$\mathbf{b} = \frac{ZS1}{2} \quad (17)$$

Fig. 7 shows the BC mho element characteristic for reverse BC faults. The figure also shows the characteristic for forward faults (dotted circle) for comparison. The polarizing quantity reduces the circle in the first quadrant for reverse faults. The mho characteristic keeps its fixed reach point, defined by the setting impedance  $Z_c$ . The element is directional, because the apparent impedance for reverse faults plots in the third quadrant.

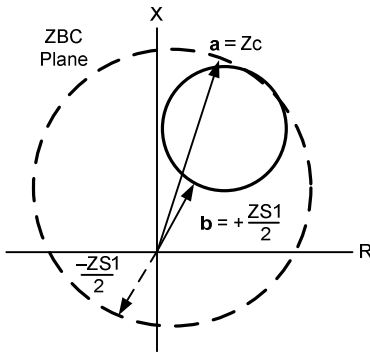


Fig. 7. BC polarized mho element characteristic for reverse BC faults.

### 3) Phase-to-Phase-to-Ground Faults

According to Table I, three distance elements correctly measure  $ZL1$  for a BCG fault: the BC, BG, and CG elements. This behavior repeats for the other two phase-to-phase-to-ground faults.

Distance relays typically enable only the phase element for phase-to-phase-to-ground faults because ground distance elements may overreach for these faults when they include fault resistance [4]. In addition, single-pole tripping (SPT) schemes should trip all three breaker poles for these multiphase faults. In our example, only the BC element is enabled for BCG faults. Hence, the  $\mathbf{a}$  and  $\mathbf{b}$  phasor expressions for BCG faults are the same as those for BC faults: (14) and (15) give  $\mathbf{a}$  and  $\mathbf{b}$  for forward faults, and (16) and (17), for reverse faults.

However, the element characteristics for BC and BCG faults are slightly different because  $IA1 = -IA2$  for BC faults in radial systems but  $IA1 \neq -IA2$  for BCG faults. As a result, the value of the  $\mathbf{b}$  phasor corresponding to BCG faults is different from the value for BC faults.

Fig. 8 shows the sequence network for a bolted BCG fault in a radial system. Equation (18) gives the  $IA1/IA2$  ratio for this fault.

$$\frac{IA1}{IA2} = -\frac{(ZS2 + ZL1) + (ZS0 + ZL0)}{ZS0 + ZL0} \quad (18)$$

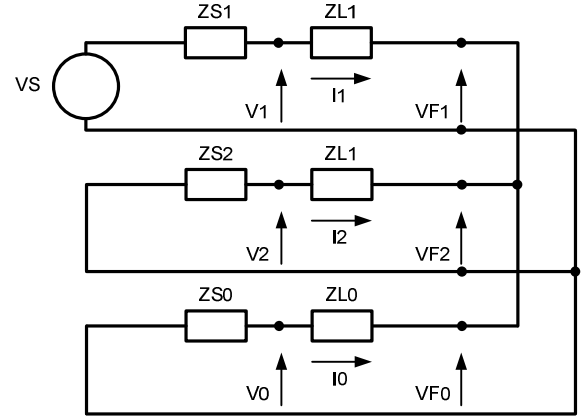


Fig. 8. Symmetrical component network for a phase-to-phase-to-ground fault.

Equation (18) shows that, when the zero-sequence impedances are much larger than the positive-sequence impedances,  $IA1/IA2$  approaches  $-1$  (as it corresponds to a BC fault) and the BC element characteristic for a BCG fault approaches that of the BC fault.

### B. Effect of Load

In radial systems and unloaded homogeneous two-source systems, the fault resistance  $R_F$  plots as a horizontal line on the apparent impedance plane [4]. The effect of load is to introduce a reactive component that effectively tilts the apparent fault impedance downwards or upwards, depending on the load flow direction. This tilt produces distance element overreach or underreach [4] [6] [8] [10].

Distance elements implemented with comparators and with the proper polarizing quantity exhibit beneficial adaptive characteristics with respect to load flow [4] [6] [10].

To illustrate this concept, consider the phase polarized mho element described by (8) and (9). The  $\mathbf{a}$  and  $\mathbf{b}$  phasors for forward faults are defined by (14) and (15). For BC faults under radial or no-load conditions,  $IA1$  and  $IA2$  are pure fault currents and  $IA1 = -IA2$ . When load flow is present,  $IA1$  includes the load current component while  $IA2$  does not, so  $IA1 \neq -IA2$ . Hence, the element characteristic differs from that for the no-load condition.

One approach to illustrate the effect of load is to use incremental quantities [11]. Using superposition, any fault current can be represented as the sum of the prefault current

and the incremental or fault current. For balanced load conditions, the prefault component appears only in the positive-sequence current, as (19) and (20) show.

$$I_1 = I_{LD} + \Delta I_1 \quad (19)$$

$$I_2 = \Delta I_2 \quad (20)$$

where:

$I_{LD}$  is the prefault load current.

$\Delta I_1$  and  $\Delta I_2$  are the incremental currents ( $\Delta I_1 = -\Delta I_2$ ).

Equation (21) provides the expression for the  $\mathbf{b}$  phasor that defines the BC element characteristic, considering the effect of load [8] [9].

$$\mathbf{b} = \frac{-ZS I_1}{2 - \frac{I_{LD}}{I A_2}} \quad (21)$$

Fig. 9 illustrates the behavior of the BC mho distance element for four combinations of  $I_{LD}$  and  $I_2$ . For the no-load condition, (21) takes the form of (13) and the mho element has the no-load Characteristic 0 in Fig. 9. Forward power flow ( $\arg(I_{LD}) = 0^\circ$ ) causes the characteristics to shift to the left (Characteristics 1 and 3). For reverse power flow ( $\arg(I_{LD}) = 180^\circ$ ), the characteristics shift to the right (Characteristics 2 and 4). For higher  $I_{LD}/I_2$  values, these shifts are more noticeable (Characteristics 3 and 4).

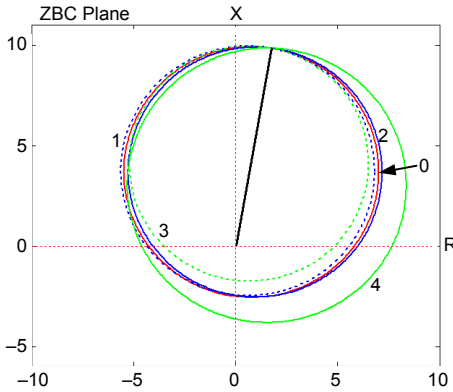


Fig. 9. BC element characteristics for different values of  $I_{LD}/I_2$ . Characteristic 0 is for no load; Characteristic 1 is for  $I_{LD}/I_2 = 0.3$ ,  $\arg(I_{LD}) = 0^\circ$ ,  $\arg(I_2) = -85^\circ$ ; Characteristic 2 is for  $I_{LD}/I_2 = 0.3$ ,  $\arg(I_{LD}) = 180^\circ$ ,  $\arg(I_2) = -85^\circ$ ; Characteristic 3 is for  $I_{LD}/I_2 = 1$ ,  $\arg(I_{LD}) = 0^\circ$ ,  $\arg(I_2) = -5^\circ$ ; and Characteristic 4 is for  $I_{LD}/I_2 = 1$ ,  $\arg(I_{LD}) = 180^\circ$ ,  $\arg(I_2) = -5^\circ$ .

Other distance elements, like the sequence current polarized reactance and resistance elements used in quadrilateral distance elements, show a more appreciable and beneficial shift in their characteristics [4] [6] [9].

In general, the characteristics on the apparent impedance plane of multiphase polarized distance elements (such as the positive-sequence polarized mho or the sequence current polarized reactance and resistance elements) are dynamic (they vary with the fault direction, the prefault power flow, or the source impedance). This dynamic behavior results from the fact that the element receives unfaulted phase information in addition to the faulted phase information that is properly reflected on the apparent impedance plane. These

characteristics are typically represented as static characteristics in manufacturer manuals for practical reasons. However, the user should be aware that the characteristics change during faults or when testing the relay.

In contrast, the characteristics on the apparent impedance plane of self-polarized distance elements (such as the mho element polarized with the voltages given in Table I and the phase current polarized reactance and resistance elements) are static. For example, the characteristic of a self-polarized mho element is a circle that crosses by the origin of coordinates and does not expand or contract during faults. As a result, this element may lack directionality for some fault locations and types. The characteristics of self-polarized distance elements do not adapt to changing power system conditions.

### C. Fault Loci

The previous sections refer to representing distance element characteristics on the impedance plane. Analyzing distance element operation for faults requires plotting on the same impedance plane the impedances measured for these faults. This is the purpose of this section. We will see that, for practical purposes, it is sometimes convenient to represent the impedance loci measured by several distance elements on the same impedance plane.

As mentioned previously, the measured impedance  $Z$  plots as a point on the impedance plane for any steady-state condition. During transient events,  $Z$  varies with time and describes a trajectory on the impedance plane.

It is possible to generate a locus composed of many steady-state measured impedance values by running multiple simulation cases for different parameter values. We use the example power system shown in Fig. 10 to show the measured impedance loci resulting from varying the fault resistance  $R_F$ .

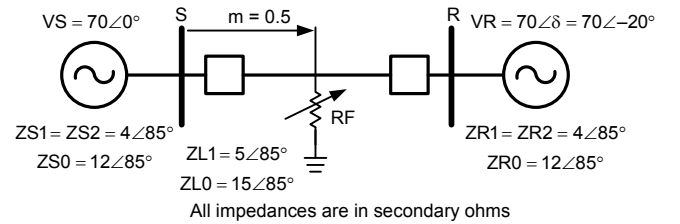


Fig. 10. Example two-source power system.

Fig. 11 through Fig. 14 show the measured impedance loci for all distance elements at Buses S and R in Fig. 10 for midline faults with different  $R_F$  values. These figures also show the  $V_1/I_1$  loci. Active power flows from S to R and reactive power flows from R to S in these examples. Fig. 11 and Fig. 12 represent AG faults. Fig. 13 and Fig. 14 represent BC faults. These figures are fault loop impedance planes.

For load conditions ( $R_F = \infty$ ), all the distance elements measure equal impedances. These impedances plot in the fourth quadrant for the Bus S elements (Fig. 11 and Fig. 13) because active power flows in the forward direction and reactive power flows in the reverse direction. For the Bus R elements (Fig. 12 and Fig. 14), the load impedance plots in the second quadrant.

As RF decreases, the impedances measured by the distance elements describe different loci. These loci end at  $RF = 0$  (bolted faults). The elements receiving faulted phase information (the AG element in Fig. 11 and Fig. 12 and the BC element in Fig. 13 and Fig. 14) correctly measure the impedance between the relay and the fault when  $RF = 0$ . The other elements measure other values of impedance, and it is possible that under some power system configurations, their apparent impedance could enter their operating region. The faulted phase selection logic should not enable these elements.

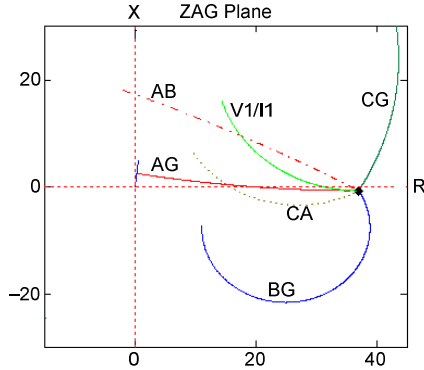


Fig. 11. Loci of the impedances measured by all distance elements at Bus S for AG faults with  $RF$  varying from  $RF = \infty$  (shown by the point) to  $RF = 0$  (forward load flow). The labels refer to distance elements.

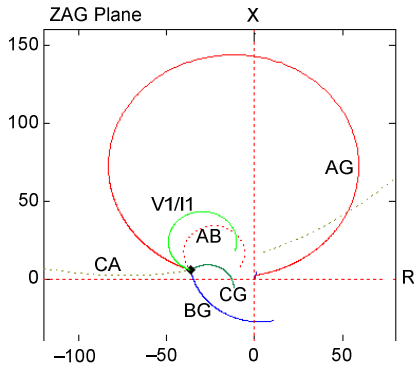


Fig. 12. Loci of the impedances measured by all distance elements at Bus R for AG faults with  $RF$  varying from  $RF = \infty$  (shown by the point) to  $RF = 0$  (reverse load flow). The labels refer to distance elements.

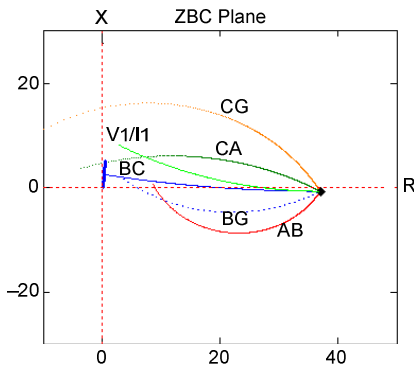


Fig. 13. Loci of the impedances measured by all distance elements at Bus S for BC faults with  $RF$  varying from  $RF = \infty$  (shown by the point) to  $RF = 0$  (forward load flow). The labels refer to distance elements.

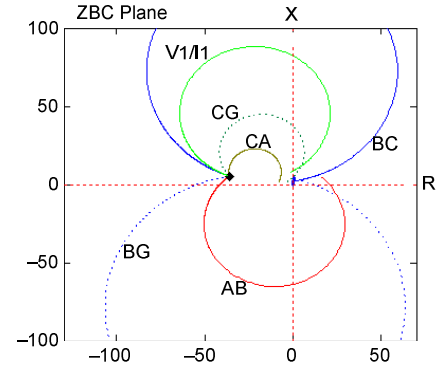


Fig. 14. Loci of the impedances measured by all distance elements at Bus R for BC faults with  $RF$  varying from  $RF = \infty$  (shown by the point) to  $RF = 0$  (reverse load flow). The labels refer to distance elements.

#### D. $k_0$ Factor Influence on the Measured Impedance

The impedance measured by ground distance elements is affected by mutual magnetic coupling in double-circuit lines. This section presents an interesting situation in which different zone elements in the same loop may measure different impedances.

Magnetic mutual induction occurs in lines mounted on multiple-circuit structures and may also occur between single-structure lines that use the same right of way. Fig. 15 shows a double-circuit structure. In this configuration, the current flowing on one line induces voltage in the other line. The magnetic flux linking with the adjacent line is mostly caused by the zero-sequence current. Positive- and negative-sequence currents add to zero and do not practically contribute to mutual coupling. Hence, mutual coupling affects ground distance elements and directional elements that use zero-sequence quantities.

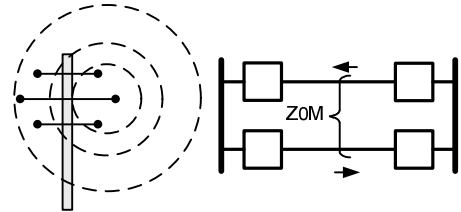


Fig. 15. In double-circuit lines, magnetic mutual coupling affects ground distance and directional elements that use zero-sequence quantities.

In parallel double-circuit line applications, the zero-sequence current that flows on each line for an external fault increases the impedance measured by the distance elements of the adjacent line [4] [12]. As a result, these elements underreach, which is acceptable for Zone 1 elements but unacceptable for Zone 2 or any other overreaching distance element. A solution to this problem is to use a large Zone 2 reach setting. A better solution is to set the Zone 2 zero-sequence compensation factor  $k_0$  to a value  $k_{0M}$  that includes the effect of mutual coupling, as (22) shows [12].

$$k_{0M} = \frac{ZL_0 - ZL_1 + Z_{0M}}{3ZL_1} \quad (22)$$

where:

$Z_{0M}$  is the zero-sequence mutual coupling impedance between the two lines.

The effect of having different zero-sequence compensation factors for Zone 1 and Zone 2 ground distance elements is that these elements measure different impedances for the same ground fault.

Consider the example 230 kV system shown in Fig. 16, which includes a parallel double-circuit line. In the relay shown in Fig. 16, Zone 1 and Zone 2 are set at 80 and 120 percent of the line impedance, respectively. From (6) and (22), we obtain  $k_0 = 0.767$  for the Zone 1 element and  $k_{0M} = 1.476$  for the Zone 2 element.

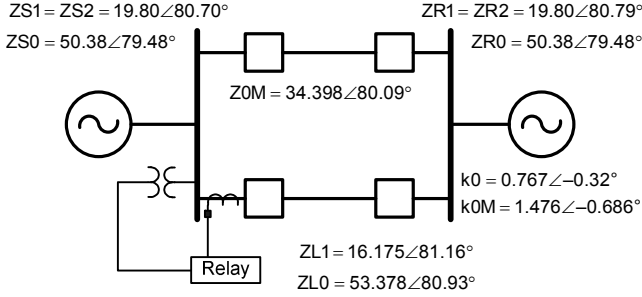


Fig. 16. Example 230 kV system that includes a double-circuit line.

Using a simulation program, an AG fault is applied at the remote right-hand-side bus. Fig. 17 illustrates the effect of using the traditional  $k_0$  value for Zone 1 and the compensated  $k_{0M}$  value for Zone 2: the AG Zone 1 element measures an impedance higher than that measured by the AG Zone 2 element. The mutual coupling compensation applied in  $k_{0M}$  places the line-end fault under the reach of the Zone 2 element. Without this compensation, the Zone 2 element would measure the same impedance as the Zone 1 element and underreach for this fault.

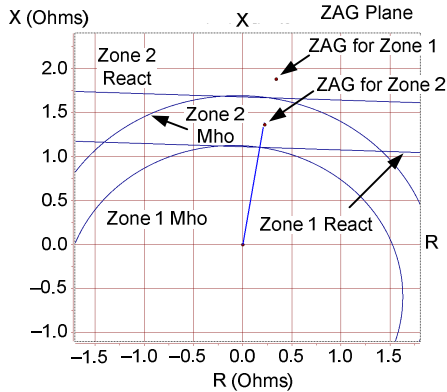


Fig. 17. Different  $k_0$  settings make Zone 1 and Zone 2 elements measure different impedances for phase-to-ground faults.

#### IV. POSITIVE-SEQUENCE (V1/I1) IMPEDANCE PLANE

Some relays include protection elements that respond to the positive-sequence voltage and current, such as power swing detection, load encroachment, and, in some cases, directional elements. The positive-sequence (V1/I1) impedance plane is used to analyze the operation of these elements.

Equation (2) shows that different combinations of voltages and currents give the same apparent impedance value for three-phase faults. This fact is also true for balanced load and power swing conditions. Hence, the impedance planes

corresponding to the six fault loops and the positive-sequence impedance plane are equivalent for any balanced power system condition. However, power swings occurring during the open-phase period following a single-pole trip make these planes different, as we show in this section.

##### A. Element Characteristics

Power system disturbances cause oscillations of machine rotors that result in power flow swings.

The impedance measured by distance elements during power swings may penetrate element operating characteristics. Power swing detection elements may be used to prevent distance element misoperation (power swing blocking) or initiate system islanding for unstable power swings (out-of-step tripping).

Power swing detection is often based on the rate of change of the measured impedance [13]. The traditional approach is to compare the measured phase or positive-sequence impedance with an element characteristic on the impedance plane. This characteristic may consist of circles, blinders, or polygons. Fig. 18 shows a characteristic composed of two concentric polygons defined on the positive-sequence impedance plane. Measuring the time that the apparent impedance stays between both polygons allows for discrimination between faults and power swings.

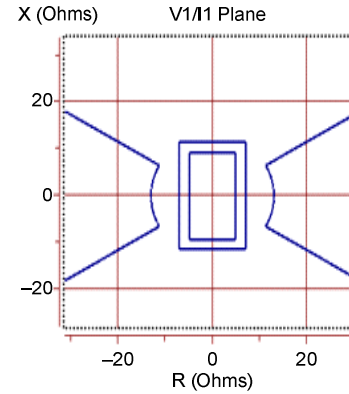


Fig. 18. Power swing detection and load-encroachment element characteristics.

Under heavy load conditions, the measured impedance may fall inside the operating characteristic of a phase distance element and cause an undesirable operation. Load-encroachment elements define two load regions on the impedance plane, as shown in Fig. 18. Under load conditions, this element blocks the operation of phase distance elements if the measured positive-sequence impedance falls into either of the load regions.

##### B. Power Swing Impedance Trajectories

The time-varying impedance measured during a power swing describes a trajectory on the impedance plane. We use the example power system in Fig. 10, with  $|V_S| = 70$  V and  $|V_R| = 65$  V, to show the measured impedance trajectories for balanced (all breaker poles closed) and unbalanced (during the single-pole-open interval in SPT schemes) power swings on different impedance planes.

Fig. 19 shows the trajectory of a balanced power swing on the positive-sequence impedance plane as the angle difference  $\delta$  between the source voltages in Fig. 10 experiences a 360-degree rotation. The trajectory crosses the line impedance, shown as a short line starting at the origin of coordinates in Fig. 19. The power swing detection element characteristic shown in Fig. 18 would appear as a small characteristic around the line impedance in Fig. 19. For this balanced power swing, the six distance elements (AG, BG, CG, AB, BC, and CA) measure exactly the same impedance as the positive-sequence element. Actually, electromechanical power swing detection relays typically use one of the combinations of phase voltages and currents given by (2) as input signals ( $V_A$  and  $I_A$  or  $V_{AB}$  and  $I_{AB}$ , for example).

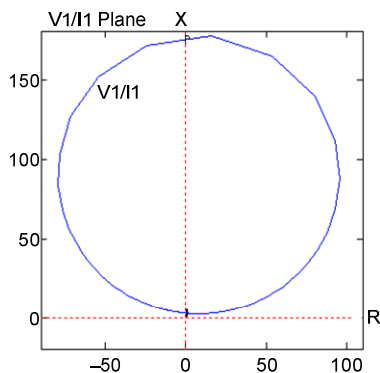


Fig. 19. The trajectory of a balanced power swing is the same on the  $V1/I1$ ,  $ZAB$ ,  $ZBC$ ,  $ZCA$ ,  $ZAG$ ,  $ZBG$ , and  $ZCG$  impedance planes.

Today, many utilities use transmission line SPT to enhance power system stability [14] [15]. SPT schemes trip only the faulted phase for single-phase-to-ground faults. After a time interval, the automatic reclosing scheme closes the open breaker pole. If the fault persists, the scheme trips all three phases and recloses again or blocks reclosing.

In SPT schemes, the open-phase interval following a single-pole trip can last for a long time. Fig. 20 shows the symmetrical component representation of an open A-phase at both terminals in a power system with the sources grounded. The power swing during the open-phase condition is unbalanced: all three sequence components of voltage and current are present.

For unbalanced power swings, the six distance elements and the positive-sequence element measure different impedances. For example, Fig. 21 shows the trajectories of an unbalanced power swing as measured by the positive-sequence, AB, BC, CA, AG, BG, and CG elements. The network in Fig. 20 was solved for particular values of  $\delta$  between 0 and 360, assuming bus-side voltage transformers.

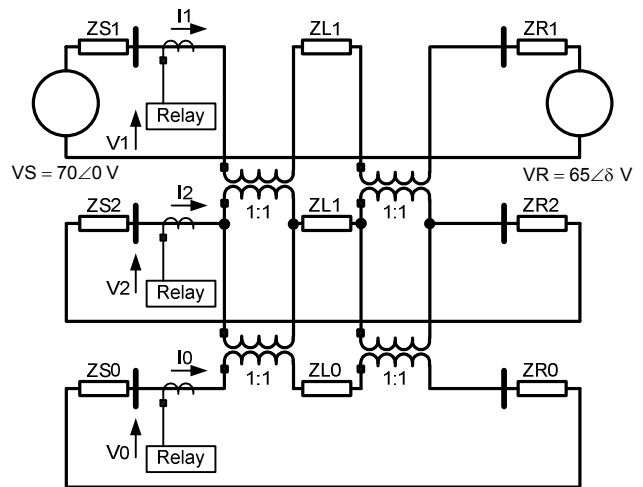


Fig. 20. A-phase open symmetrical component network used to find the impedance trajectories during a power swing.

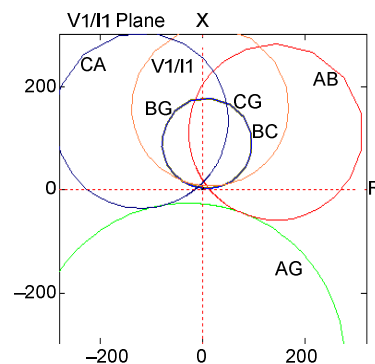


Fig. 21. The trajectories of unbalanced power swings are different on the  $V1/I1$ ,  $ZAB$ ,  $ZBC$ ,  $ZCA$ ,  $ZAG$ ,  $ZBG$ , and  $ZCG$  impedance planes. The labels refer to distance elements.

Fig. 21 shows that the positive-sequence,  $ZBC$ ,  $ZBG$ , and  $ZCG$  trajectories have the same shape as that in Fig. 19. However, the trajectories measured by the AB, CA, and AG elements, which measure A-phase information with Pole A open in this example, are significantly shifted. The characteristics of the elements that receive information from the open phase are also shifted when the B- or C-phase is open during the power swing.

When using line-side voltage transformers, voltage measurements may be corrupted during the open-phase period by the oscillating transients because of the line inductance and capacitance [16]. In response to the open-phase condition, the relay typically eliminates this voltage measurement from the positive-sequence voltage calculation to avoid errors [17]. For example, (23) provides the  $V1$  calculation when the A-phase is open.

$$V1 = \frac{1}{3}(0 + aV_B + a^2V_C) \quad (23)$$

Fig. 22 shows the positive-sequence impedance trajectories for a balanced power swing (the same as that in Fig. 19) and an unbalanced power swing, with  $V1$  calculated using bus-side and line-side voltage. When considered in the part of the impedance plane where the power swing characteristics are placed, all the trajectories have the same shape and no significant shift.

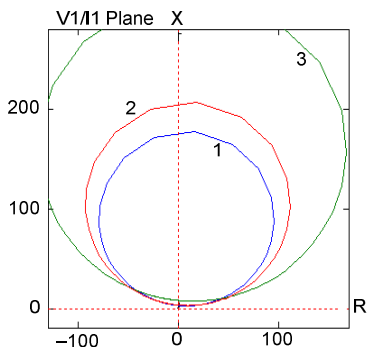


Fig. 22. Power swing trajectories for a balanced power swing (Trajectory 1) and for unbalanced power swings, using line-side (Trajectory 2) and bus-side (Trajectory 3) voltage to calculate  $V1$ .

## V. NEGATIVE-SEQUENCE ( $V2/I2$ ) AND ZERO-SEQUENCE ( $V0/I0$ ) IMPEDANCE PLANES

Some relays include directional elements that respond to the negative- or zero-sequence voltage and current. The negative-sequence ( $V2/I2$ ) or zero-sequence ( $V0/I0$ ) impedance planes should be used to analyze the operation of these elements.

### A. Element Characteristics

Traditional directional elements compare the angle between a polarizing quantity ( $V2$  or  $V0$ , for example) and an operating quantity ( $I2$  or  $I0$ ). An implementation of negative- and zero-sequence directional elements calculates an impedance scalar quantity. For example, the negative-sequence element calculates the scalar quantity  $z2$  using (24) [4] [7], which is the projection of  $V2/I2$  on a straight line that has the line impedance angle ( $\angle ZL1$ ).

$$z2 = \frac{\text{Re}(V2(I2 e^{j\angle ZL1})^*)}{|I2|^2} = \left| \frac{V2}{I2} \right| \cos\left(\angle \frac{V2}{I2} - \angle ZL1\right) \quad (24)$$

where:

\* represents the phasor complex conjugate operation.

This element compares  $z2$  against two thresholds. If  $z2$  is less than a forward fault threshold, the element declares a forward fault. If  $z2$  is greater than a reverse fault threshold, the element declares a reverse fault. Equation (25) gives the forward threshold and (26), the reverse threshold (for  $Z2F > 0$  and  $Z2R > 0$ ).

$$1.25 Z2F - 0.25 \left| \frac{V2}{I2} \right| \quad (25)$$

$$0.75 Z2R + 0.25 \left| \frac{V2}{I2} \right| \quad (26)$$

where:

$Z2F$  and  $Z2R$  are relay settings.

Equating (24) to (25) and (26) and solving for  $V2/V1$ , we obtain (27) and (28), which define the forward and reverse operating characteristics on the  $V2/I2$  plane shown in Fig. 23.

$$\left| \frac{V2}{I2} \right| = \frac{1.25 Z2F}{\cos\left(\angle \frac{V2}{I2} - \angle ZL1\right) + 0.25} \quad (27)$$

$$\left| \frac{V2}{I2} \right| = \frac{0.75 Z2R}{\cos\left(\angle \frac{V2}{I2} - \angle ZL1\right) - 0.25} \quad (28)$$

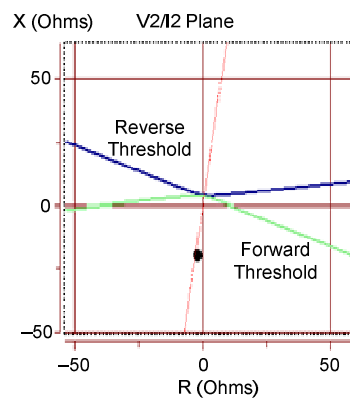


Fig. 23. Negative-sequence directional element characteristics.

The forward operating region is located below the forward characteristic, and the reverse operating region is located above the reverse characteristic.

Similarly, the zero-sequence directional element calculates an impedance scalar quantity  $z0$  and compares it against forward and reverse thresholds.

### B. Measured Impedances

Fig. 24 shows the negative-sequence network for a forward unbalanced fault in a two-source system. For any forward fault location (any  $m$  value), the directional element measures the negative-sequence impedance of the equivalent system behind the relay, as (29) and Fig. 23 show.

$$\frac{V_2}{I_2} = -Z_{S2} \quad (29)$$

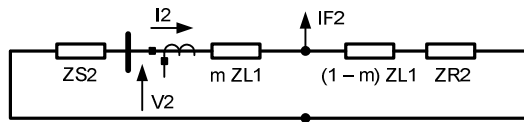


Fig. 24. Negative-sequence network for a forward unbalanced fault in a two-source system.

A similar analysis shows that, for all reverse unbalanced faults, the directional element measures the negative-sequence impedance of the equivalent system in front of the relay.

$$\frac{V_2}{I_2} = +(Z_{L1} + Z_{R2}) \quad (30)$$

The characteristics of sequence directional elements are frequently shown on the same impedance planes as those used for distance elements. An example is the quadrilateral distance element characteristic, in which a directional element characteristic, generally represented as a straight line crossing by the origin of coordinates, shows the forward direction with respect to the relay location.

Consider, for illustration, a line with a series capacitor (Fig. 25). This capacitor does not modify the negative-sequence impedance measurement (29) for forward faults. The negative of the source impedance plots on the element operating region. However, the series capacitor and the protected line impedances plot on the ZBC plane, as shown in Fig. 26. A fault right after the capacitor plots at Point F, which conveys the idea of a reverse fault on the ZBC plane. However, the negative-sequence directional element responds well to this forward fault. The key conclusion is that the characteristics of negative-sequence (or zero-sequence) directional elements cannot be represented on the impedance planes used for distance elements.

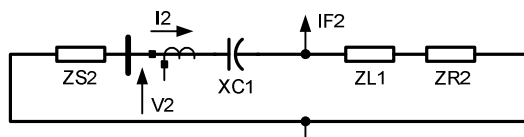


Fig. 25. A series capacitor in the protected line does not affect the negative-sequence impedance measurement for forward faults.

Fig. 27 shows the proper way to represent a quadrilateral distance element characteristic. Fig. 27 shows only three boundaries. The top boundary (X) is a reactance line, which limits the reach for forward faults. The right boundary (Right) limits the resistive reach on the forward power flow direction. Likewise, the left boundary (Rleft) limits the resistive reach on the reverse power flow direction. The characteristic of a

sequence directional element should not be represented on this impedance plane.

As mentioned previously, the characteristics of the reactance and resistance elements are static only if these elements are self-polarized. The characteristics of sequence current polarized reactance and resistance elements are dynamic.

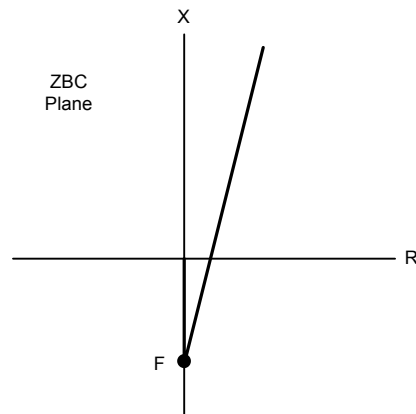


Fig. 26. A series capacitor in front of the relay plots as a negative reactance on the ZBC plane, which gives the idea that a directional element will not operate for a fault beyond the capacitor.

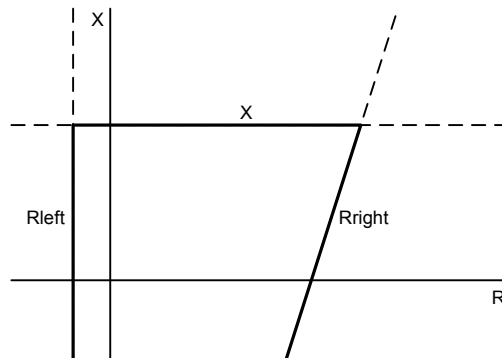


Fig. 27. Proper way to represent a quadrilateral distance element characteristic.

## VI. FIELD CASE EXAMPLE

A real-life power system event serves to illustrate some of the concepts discussed in this paper. This section shows that different impedance planes can be used to analyze a power system event.

Fig. 28 shows the oscillogram recorded by a relay installed on a 115 kV line as part of a permissive overreaching transfer trip (POTT) directional comparison scheme with SPT logic. For an external BG fault, this relay incorrectly received the permissive signal from the remote terminal, caused the opening of the B-phase of the line, and successfully reclosed. The fault occurred on a 69 kV line separated from the relay location by the 115 kV line, three autotransformers, and a long 230 kV line.

Section 1 in Fig. 28 shows the BG fault. This external fault was correctly detected as a forward fault by the local relay of the 115 kV line. However, the remote relay did not detect the fault because of a wrong setting and echoed the permissive tripping signal sent by the local relay. As a result, the local

relay tripped, opening the B-phase of the 115 kV line. Section 2 in the oscillogram shows the resulting unbalanced power swing, which ends when the faulted line protection trips to clear the fault. Practically at the same time, the 115 kV line protection scheme successfully recloses the B-phase, and a balanced power swing (Section 3 in Fig. 28) starts. This power swing eventually damps out, and the system continues to operate normally.

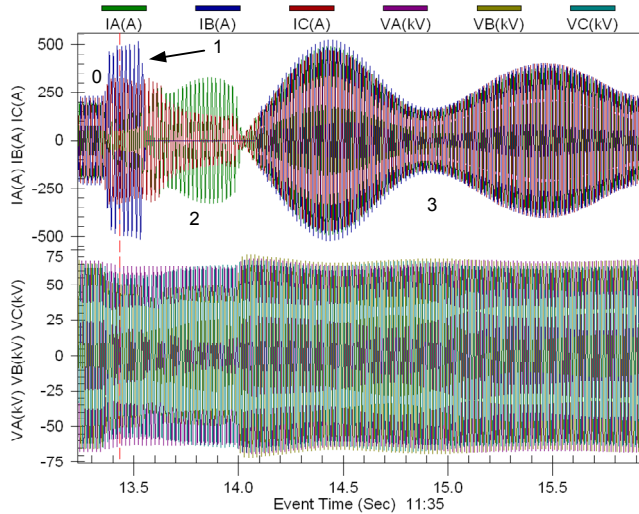


Fig. 28. Oscillogram recorded by an unfaulted 115 kV line relay. Section 0 is the pre-fault condition; Section 1 is an external BG fault followed by an incorrect single-pole trip; Section 2 is an unbalanced power swing during the B-phase open period; and Section 3 is a balanced power swing after faulted line tripping and unfaulted line B-phase reclosing.

Fig. 29 shows the impedance measured by the local BG ground distance elements on the ZBG plane. The fault impedance plots far away from the element characteristics and shows an apparent fault resistance value of approximately 8 secondary ohms. The polarized mho element characteristics exhibit a significant expansion for this forward fault. These elements did not operate.

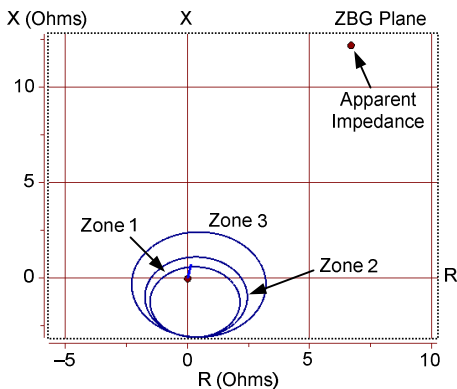


Fig. 29. ZBG plane representation of the external BG fault (Section 1 in Fig. 28).

Fig. 30 shows the impedance measured by the local negative-sequence ground directional element. The negative-sequence impedance equals the source impedance behind the relay and plots inside the element forward operating region.

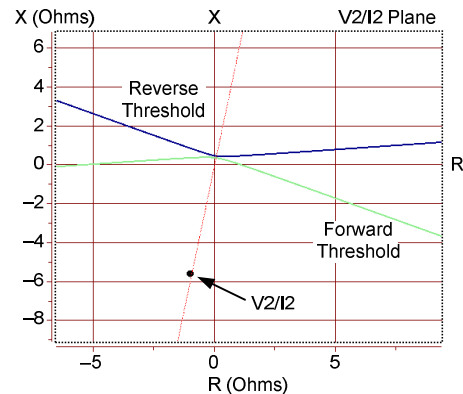


Fig. 30. Negative-sequence plane representation of the external BG fault (Section 1 in Fig. 28).

Fig. 31 represents the event on the positive-sequence impedance plane. It also shows the power swing detection element characteristic. Point 0 represents the pre-fault condition. Point 1 is the fault point. The impedance trajectory between Point 0 and Point 1 represents the relay filtering transient process triggered by the fault. Trajectory 2 that starts at Point 1 is the unbalanced power swing during the B-phase open period. This trajectory leaves the impedance plane on the right side of the figure and returns on the left side (Trajectory 3), already representing a balanced power swing. After some oscillations close to the left side of the power swing detection element characteristic, this trajectory eventually ends close to the initial operation Point 0.

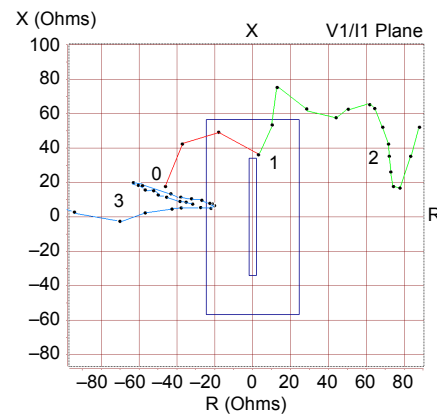


Fig. 31. Positive-sequence plane representation of the event shown in Fig. 28. Point 0 is the pre-fault condition; Point 1 is a BG fault; Trajectory 2 is an unbalanced power swing (B-phase open); and Trajectory 3 is a balanced power swing.

This example illustrates the use of different impedance planes to analyze the operation of protection elements with different input signals.

### VII. CONCLUSION

From the study of impedance planes in this paper, the following can be concluded:

- Distance and directional elements perform signal phase comparison to create operating characteristics. The impedance plane serves to analyze the operation of these elements by superimposing the characteristic and the impedance measured by the element.

- Two impedance planes can be used for phase and ground distance elements: the apparent impedance plane (defined by the ratio of the element input signals) and the fault loop impedance plane (defined by the ratio of the signals corresponding to the faulted phases).
- The apparent impedance plane allows the analysis of element operation for faults, power swings, and load conditions.
- Other planes used in protective relaying include the positive-, negative-, and zero-sequence impedance planes and the current-ratio plane.
- Analyzing the operation of protection elements with different input signals requires different impedance planes. For example, the characteristic of a negative- or zero-sequence directional element should not be represented on the same plane as the characteristics of phase or ground distance elements.
- The characteristics on the apparent impedance plane of self-polarized distance elements are static (do not vary with the fault direction, the prefault power flow, or the source impedance).
- The characteristics on the apparent impedance plane of multiphase polarized distance elements (such as the positive-sequence polarized  $m\Omega$  or the sequence current polarized reactance and resistance elements) are dynamic (they vary with the fault direction, the prefault power flow, or the source impedance).
- For practical purposes, it is sometimes convenient to use the same impedance plane to represent characteristics and impedances measured by distance elements from different phases (see Fig. 11 through Fig. 14 and Fig. 21, for example). Care should be exercised during this process and when analyzing the results.
- The use of tools that allow the visualization of the different protective relaying planes facilitates the analysis of relaying element operation (in particular, of the multiphase polarized distance elements) during power system events.

### VIII. REFERENCES

- [1] C. R. Mason, *The Art and Science of Protective Relaying*. John Wiley and Sons, New York, NY, 1956.
- [2] A. R. van C. Warrington, *Protective Relays: Their Theory and Practice*, Vol. 1. Chapman and Hall Ltd., London, England, 1962.
- [3] V. Cook, *Analysis of Distance Protection*. Research Studies Press Ltd., Letchworth, England, 1985.
- [4] H. J. Altuve Ferrer and E. O. Schweitzer, III (eds.), *Modern Solutions for Protection, Control, and Monitoring of Electric Power Systems*. Schweitzer Engineering Laboratories, Inc., Pullman, WA, 2010.
- [5] E. O. Schweitzer, III, "New Developments in Distance Relay Polarization and Fault Type Selection," proceedings of the 16th Annual Western Protective Relay Conference, Spokane, WA, October 1989.
- [6] E. O. Schweitzer, III and J. Roberts, "Distance Relay Element Design," proceedings of the 46th Annual Conference for Protective Relay Engineers, College Station, TX, April 1993.
- [7] J. Roberts and A. Guzmán, "Directional Element Design and Evaluation," proceedings of the 21st Annual Western Protective Relay Conference, Spokane, WA, October 1994.
- [8] F. Calero, "Distance Elements: Linking Theory With Testing," proceedings of the 62nd Annual Conference for Protective Relay Engineers, College Station, TX, March 2009.
- [9] F. Calero, A. Guzmán, and G. Benmouyal, "Adaptive Phase and Ground Quadrilateral Distance Elements," proceedings of the 36th Annual Western Protective Relay Conference, Spokane, WA, October 2009.
- [10] J. Roberts, A. Guzmán, and E. O. Schweitzer, III, " $Z = V/I$  Does Not Make a Distance Relay," proceedings of the 20th Annual Western Protective Relay Conference, Spokane, WA, October 1993.
- [11] G. Benmouyal and J. Roberts, "Superimposed Quantities: Their True Nature and Application in Relays," proceedings of the 26th Annual Western Protective Relay Conference, Spokane, WA, October 1999.
- [12] F. Calero, "Mutual Impedance in Parallel Lines – Protective Relaying and Fault Location Considerations," proceedings of the 34th Annual Western Protective Relay Conference, Spokane, WA, October 2007.
- [13] D. A. Tziouvaras and D. Hou, "Out-of-Step Protection Fundamentals and Advancements," proceedings of the 30th Annual Western Protective Relay Conference, Spokane, WA, October 2003.
- [14] F. Calero and D. Hou, "Practical Considerations for Single-Pole-Trip Line-Protection Schemes," proceedings of the 31st Annual Western Protective Relay Conference, Spokane, WA, October 2004.
- [15] V. H. Serna, J. C. Rivera, H. E. Prado, H. J. Altuve, D. Sánchez, and J. Gallegos, "Transmission Line Single-Pole Tripping: Field Experience in the Western Transmission Area of Mexico," proceedings of the 37th Annual Western Protective Relay Conference, Spokane, WA, October 2010.
- [16] D. Hou, A. Guzmán, and J. Roberts, "Innovative Solutions Improve Transmission Line Protection," proceedings of the 24th Annual Western Protective Relay Conference, Spokane, WA, October 1997.
- [17] A. Guzmán, J. Mooney, G. Benmouyal, and N. Fischer, "Transmission Line Protection System for Increasing Power System Requirements," proceedings of the 55th Annual Conference for Protective Relay Engineers, College Station, TX, April 2002.

### IX. BIOGRAPHIES

**Fernando Calero** received his BSEE in 1986 from the University of Kansas, his MSEE in 1987 from the University of Illinois (Urbana-Champaign), and his MSEPE in 1989 from the Rensselaer Polytechnic Institute. From 1990 to 1996, he worked in Coral Springs, Florida, for the ABB relay division in the support, training, testing, and design of protective relays. Between 1997 and 2000, he worked for Itec Engineering, Florida Power and Light, and Siemens. In 2000, Mr. Calero joined Schweitzer Engineering Laboratories, Inc. and presently is a senior automation systems engineer.

**Héctor J. Altuve Ferrer** received his BSEE degree in 1969 from the Central University of Las Villas in Santa Clara, Cuba, and his Ph.D. in 1981 from Kiev Polytechnic Institute in Kiev, Ukraine. From 1969 until 1993, Dr. Altuve served on the faculty of the Electrical Engineering School at the Central University of Las Villas. From 1993 to 2000, he served as professor of the Graduate Doctoral Program in the Mechanical and Electrical Engineering School at the Autonomous University of Nuevo León in Monterrey, Mexico. In 1999 through 2000, he was the Schweitzer Visiting Professor in the Department of Electrical Engineering at Washington State University. Dr. Altuve joined Schweitzer Engineering Laboratories, Inc. in January 2001, where he is currently a distinguished engineer and director of technology for Latin America. He has authored and coauthored more than 100 technical papers and several books and holds four patents. His main research interests are in power system protection, control, and monitoring. Dr. Altuve is an IEEE senior member.